

J.E. Rice, Y.A. Podpaly, M.L. Reinke, R. Mumgaard, S.D. Scott, S. Shiraiwa,
G.M. Wallace, B. Chouli, C. Fenzi-Bonizec, M.F.F. Nave, P.H. Diamond,
C. Gao, J.W. Hughes, P.T. Bonoli, L. Delgado-Aparicio, L.-G. Eriksson,
C. Giroud, R.S. Granetz, M.J. Greenwald, A.E. Hubbard, I.H. Hutchinson,
J.H. Irby, K. Kirov, J. Mailloux, E.S. Marmar, R.R. Parker, S.M. Wolfe
and JET EFDA contributors

Effects of Magnetic Shear on Toroidal Rotation in Tokamak Plasmas with LHCD

“This document is intended for publication in the open literature. It is made available on the understanding that it may not be further circulated and extracts or references may not be published prior to publication of the original when applicable, or without the consent of the Publications Officer, EFDA, Culham Science Centre, Abingdon, Oxon, OX14 3DB, UK.”

“Enquiries about Copyright and reproduction should be addressed to the Publications Officer, EFDA, Culham Science Centre, Abingdon, Oxon, OX14 3DB, UK.”

The contents of this preprint and all other JET EFDA Preprints and Conference Papers are available to view online free at www.iop.org/Jet. This site has full search facilities and e-mail alert options. The diagrams contained within the PDFs on this site are hyperlinked from the year 1996 onwards.

Effects of Magnetic Shear on Toroidal Rotation in Tokamak Plasmas with LHCD

J.E. Rice¹, Y.A. Podpaly¹, M.L. Reinke¹, R. Mumgaard¹, S.D. Scott², S. Shiraiwa¹,
G.M. Wallace¹, B. Chouli³, C. Fenzi-Bonizec³, M.F.F. Nave⁴, P.H. Diamond⁵,
C. Gao¹, J.W. Hughes¹, P.T. Bonoli¹, L. Delgado-Aparicio², L.-G. Eriksson⁶,
C. Giroud⁷, R.S. Granetz¹, M.J. Greenwald¹, A.E. Hubbard¹, I.H. Hutchinson¹,
J.H. Irby¹, K. Kirov⁷, J. Mailloux⁷, E.S. Marmor¹, R.R. Parker¹, S.M. Wolfe¹
and JET EFDA contributors

JET-EFDA, Culham Science Centre, OX14 3DB, Abingdon, UK

¹*PSFC MIT, Cambridge, Massachusetts 02139, USA*

²*PPPL, Princeton, New Jersey 08543, USA*

³*CEA-Cadarache, 13108 St.-Paul-lez-Durance, France*

⁴*Associação EURATOM/IST, Universidade Técnica de Lisboa, 1049-001, Lisbon, Portugal*

⁵*CMTFO, UCSD, San Diego, California 92903, USA*

⁶*European Commission, Research Directorate General, B-1049 Brussels, Belgium*

⁷*CCFE/EURATOM Fusion Association, Abingdon OX14 3DB, UK*

** See annex of F. Romanelli et al, "Overview of JET Results",
(24th IAEA Fusion Energy Conference, San Diego, USA (2012)).*

ABSTRACT

Application of lower hybrid current drive (LHCD) in tokamak plasmas can induce both co- and counter-current directed changes in toroidal rotation, depending on the core magnetic shear, \hat{s} . For discharges with $\hat{s} > 1$, rotation increments in the counter-current direction are observed. If the LH driven current is sufficient to suppress saw-teeth and reduce the central \hat{s} below unity, the core toroidal rotation change is in the co-current direction. This change in sign of the rotation increment is consistent with a change in sign of the residual stress (the divergence of which constitutes an intrinsic torque that drives the flow) through its dependence on \hat{s} .

INTRODUCTION

The benefits of rotation and flow shear for tokamak performance are well known. Toroidal rotation is often driven externally through neutral beam injection, but beam torque is expected to be small in future fusion devices, so other methods for rotation drive are necessary. One possibility is to take advantage of self-generated flow in enhanced confinement regimes [1], but this process relies on plasma performance, which makes for a complicated control knob. Another approach is to utilize radio frequency waves (ion cyclotron, electron cyclotron and lower hybrid), although the mechanisms of direct generation of rotation are not well understood. ICRF mode conversion flow drive has been demonstrated [2] and rotation effects due to ECH have been seen [3]. Toroidal rotation changes due to lower hybrid (LH) waves have also been observed [4, 5, 6, 7, 8, 9, 10], with velocities in both the co- and counter-current directions. Even in plasmas with good core absorption of LH waves, the mechanism for rotation drive is not clear. Candidates include direct momentum input from the waves (calculated to be low [7]), electron orbit loss [4], trapped electron pinch effects [11], resonant electron radial drift [12, 13], and less direct causes such as the turbulent equipartition pinch [8] or through modification of the q profile [9, 10]. A challenge of these accounts is to explain the rotation changes observed in both directions. To this end, this paper compares the response of rotation to the q profile in Alcator C-Mod, Tore Supra and JET.

Shown in Figure 1 is a comparison of core toroidal rotation velocity time histories for two 5.4T LHCD ($n_{||} = 1.6$) discharges with line averaged density $\langle n_e \rangle = 0.7 \times 10^{20} / \text{m}^3$ from Alcator C-Mod ($R = 0.67\text{m}$, $a \sim 0.21\text{m}$), and with plasma currents of 0.91MA ($q_{95} = 3.7$) and 0.42MA ($q_{95} = 7.7$). For the higher current case, there was change in core rotation (from the initial +20km/s) in the counter-current direction of $\sim 30\text{km/s}$, which evolved on a current relaxation time scale (100s of ms), considerably longer than the momentum confinement time (10s of ms). For the lower current case, there was an increment of $\sim 30\text{km/s}$ in the co-current direction, from an initial velocity of -50km/s . The 0.91MA discharge had sawtooth oscillations throughout the duration of the LHRF wave injection, whereas the sawteeth in the 0.42MA plasma were stabilized beginning at 0.97s.

Velocity profiles determined from x-ray imaging spectroscopy for high and low plasma current discharges with $\langle n_e \rangle = 0.7 \times 10^{20} / \text{m}^3$, before and during injection of ~ 0.8 MW of LHCD power, are shown in Figure 2. For the 0.71MA Ohmic target plasma, the profile is relatively flat, with a co-

current velocity around +25km/s across the profile. For the 0.42MA Ohmic target plasma, the profile is strongly counter-current in the core and has a steep gradient region just inside of the mid radius. The profiles are similar during the LHCD injection, becoming slightly counter current in the core. The particular shape changes of the high current discharge, which changes sign in the core region, suggest that these profiles are not the result of a momentum pinch effect. There is no change in the profiles outside of the mid radius ($r/a \sim 0.55$) with LHCD [5, 6]. Similar rotation profile behavior has been seen in JET [7, 10] and Tore Supra LHCD plasmas. This anchoring of the profiles in the vicinity of the mid radius is reminiscent of what is observed during Ohmic rotation reversal [14].

It is important to understand what causes these bi-directional rotation changes with LHCD. This observed bi-directionality seems to rule out direct momentum input, since the waves are launched in the same direction in both cases. The input torque from LH waves [7], $Rn_{\parallel}PLH/c \sim 0.002\text{Nm}$ (for the cases shown in Figure 1), is directed in the counter-current direction. To address this rotation increment direction issue, an examination of rotation characteristics has been performed during a dedicated shot by shot plasma current scan.

The change/increment in the central rotation velocity (the difference in the time averaged velocity at the end of the LHCD pulse, 1.2-1.3s, and the pre-LHCD phase, 0.7–0.8s) as a function of plasma current, for a series of similar 5.4 T C-Mod discharges with $n_e = 0.7 \times 10^{20}/\text{m}^3$ and LHCD power between 0.75 and 0.9MW, is shown in the bottom panel of Figure 3. The *change* in steady state rotation varies strongly with plasma current, going from $\sim +30\text{km/s}$ at the lowest current (0.32MA, $q_{95} = 9.6$) to around -25km/s at the highest current (0.91MA, $q_{95} = 3.7$). There is a stagnation point for $I_p \sim 0.6\text{MA}$ ($q_{95} = 5.5$) for these particular target plasma conditions, where application of 0.8MW of LHCD power has little effect on the central rotation. The zero crossing point for these discharges is very close to the intrinsic rotation reversal critical density and current [14, 15, 16], suggesting a possible connexion between this bi-directional rotation change with LHCD and intrinsic Ohmic rotation reversals. As shown in the top panel of Figure 3, the intrinsic rotation velocity of the Ohmic (pre-LHCD) target plasma also depends strongly on the plasma current [16, 10] in this current scan. The core toroidal rotation varies from -60km/s at the lowest I_p to $+20\text{km/s}$ at the highest, and the intrinsic Ohmic rotation switches direction at $\sim 0.7\text{MA}$ for this electron density and magnetic field, an example of the rotation reversal phenomenon [17, 14, 15, 16]. The rotation profile anchoring shown in Figure 2 and the similarity between the LHCD rotation bi-directionality and intrinsic Ohmic rotation reversal critical points suggests that the two phenomena may be related.

The cause of the flip in rotation direction for Ohmic plasmas is thought to be due to a reversal in sign of the residual stress [18], Π_r , due to a change of domination from trapped electron modes (TEMs) to ion temperature gradient (ITG) modes above a critical collisionality (ν_*) [14, 15, 16]. Π_r is the component of the momentum flux not proportional to the velocity or its gradient, whose sign depends on the underlying turbulent modes. The divergence of Π_r is the intrinsic torque density. Π_r also is a function of the gradient of the current density profile [19, 18, 20, 21, 22], and in principle can switch sign through changes in the current density profile by externally driven current *via* LH waves.

Evidence for the role of the current density profile is suggested by changes in sawtooth behavior. LHCD plasmas which had sawtooth oscillations showed counter-current velocity increments, while in the co-current increment discharges, the sawteeth were suppressed due to a significant change in the q profile. Table 1 summarizes the sawtooth behavior for a database of 243 low density target C-Mod plasmas with LHCD. No co- increment discharges exhibited sawtooth oscillations while all sawtoothing discharges underwent counter-current rotation changes. Only a few counter- increment plasmas were without sawteeth. LHCD discharges without sawteeth also experienced co-current rotation increments in JT-60U, EAST [8], JET [10] and Tore Supra. A summary of the LHCD rotation parameters from various tokamaks is shown in Table 2. The first column gives the rotation increment direction following LHCD.

Current density profiles for C-Mod plasmas have been determined from EFIT calculations constrained by MSE observations [23, 24] enabled by a diagnostic neutral beam. The rotational transform q and magnetic shear ($\hat{s} = r/q \partial q/\partial r$) profiles, for three discharges from Figure 3 with plasma currents of 0.32, 0.58 and 0.91MA, evaluated at 1.14s, are shown in Figure 4. For the 0.91MA plasma (which was sawtoothing throughout the LHCD pulse), the q profile (top frame) increases monotonically, with q_0 well below 1 at the magnetic axis. The zero crossing at 0.75m is consistent with the measured sawtooth inversion radius. For the 0.32MA case, the q profile is flat in the core, with a value just under 2; for the 0.58MA plasma, $q_0 \sim 1.3$. This is consistent with the lack of sawtooth oscillations for these latter two discharges. Another difference between these cases is the magnetic shear (bottom frame); for the 0.91MA plasma, \hat{s} in the core was about 2.5, for the 0.58MA case \hat{s} was constant near unity, while for the 0.32MA discharge, \hat{s} was near 0. Interestingly, all three \hat{s} profiles converge near the mid radius, which is close to the rotation profile stagnation point shown in Figure 2. For the low current case, \hat{s} hovers ~ 0 which gives rise to an unstable magnetic shear scale length L_s ($\equiv R_0 q/\hat{s}$) inside $R = 0.75\text{m}$ ($r/a \sim 0.3$). For the 0.91MA plasma, the central L_s was $\sim 0.2\text{m}$, and $\sim 1\text{m}$ for the 0.58MA discharge.

The connexion between the magnetic shear and direction of rotation increment is illustrated in Figure 5 where the change in the core rotation velocity with LHCD is shown as a function of the average value of \hat{s} inside of $r/a \sim 0.3$. There is an abrupt change in the LHCD rotation increment, going from co- to counter-, near $\hat{s} \sim 1$, exhibiting a threshold behavior. Typical error bars are shown. A related threshold is seen as a function of the central rotational transform, as is illustrated in Figure 6, where the change in core rotation frequency is shown depending on q_0 . The null in $\Delta\omega$ is close to $q_0 \sim 1$. The use of the rotation frequency allows for direct comparison with the results from other devices; also shown in Figure 6 are points from EAST [8], JET [10] and Tore Supra, which fit well with those from C-Mod. These points generally occupy two quadrants in this operational space: counter-current rotation increments for plasmas with $q_0 < 1$ and co-current for $q_0 > 1$.

These changes in the q profiles are significant, because the structure of the residual stress, Π_r [19, 20, 21] (which gives rise to an intrinsic torque *via* $\nabla \cdot \Pi_r$), and the turbulent acceleration [25], both depend sensitively on the magnetic shear, \hat{s} , and mode structure *via* ion-acoustic coupling. In

particular, both these drivers of intrinsic rotation require symmetry breaking, so as to set a finite value of $\langle k_{\perp} k_{\parallel} |\hat{\Phi}_k|^2 \rangle$, necessary for intrinsic torque. Here the bracket refers to a spectral average. To this end, the intrinsic torque can change noticeably [26] as q' and \hat{s} drop, and q'' increases. Furthermore, the intrinsic torque for the normal magnetic shear and ‘flat q ’ cases can differ significantly, although the case may be understated. For weak shear (flat q profiles), non-resonant modes become increasingly important. Recent work [27] has characterized the structure of non-resonant modes and noted that they are best thought of as extended convective cells, with little, if any, similarity to the familiar resonant modes. Further studies [28] have revealed that these non-resonant modes make a substantial contribution to the turbulent heat flux. Thus, there is every reason to expect that the non-resonant modes play an important role in the non-diffusive radial flux of toroidal momentum and the associated Reynolds stress $\langle \tilde{v}_r \tilde{v}_\phi \rangle$. Studies of the effect of non-resonant modes on momentum transport are ongoing and will be discussed in future publications. For now, it should be emphasized that the change in intrinsic torque as LHCD induced current increases and $q(r)$ flattens is quite likely related to the contributions of non-resonant modes. Previous work on turbulence driven intrinsic torque has ignored the effect of non-resonant modes.

In summary, LH waves have been introduced into L-mode target plasmas, resulting in velocity changes in both the co- and counter-current directions. For observations from several tokamaks with LHCD, the rotation direction depends on the resulting changes in the q profile, with co- rotation increments seen in plasmas with $q_0 > 1$, and counter-current changes with $q_0 < 1$. This effect likely results from changes in the intrinsic torque (divergence of the residual stress) through changes in the current density profile.

ACKNOWLEDGEMENTS

The authors thank M.Yoshida, S.Koide and Y.Shi for information regarding LHCD rotation and the Alcator C-Mod operations and LH groups for expert running of the tokamak. Work supported at MIT by DoE Contract No. DE-FC02-99ER54512 and in part by an appointment to the US DOE Fusion Energy Postdoctoral Research Program administered by ORISE.

REFERENCES

- [1]. J.E. Rice et al., 2007 Nuclear Fusion **47** 1618.
- [2]. Y. Lin et al., 2008 Physical Review Letters **101** 235002.
- [3]. M. Yoshida et al., 2009 Physical Review Letters **103** 065003.
- [4]. Y. Sakamoto et al., 2006 Plasma Physics and Controlled Fusion **48** A63.
- [5]. A. Ince-Cushman et al., 2009 Physical Review Letters **102** 035002.
- [6]. J.E. Rice et al., 2009 Nuclear Fusion **49** 025004.
- [7]. L.-G. Eriksson et al., 2009 Plasma Physics and Controlled Fusion **51** 044008.
- [8]. Yuejiang Shi et al., 2011 Physical Review Letters **106** 235001.
- [9]. J.E. Rice et al., 2013, 'Effects of LHRF on toroidal rotation in Alcator C-Mod plasmas' submitted to Nuclear Fusion.
- [10]. M.F.F. Nave et al., 2013, 'Scalings of spontaneous rotation in the JET tokamak' submitted to Nuclear Fusion.
- [11]. Z. Gao et al., 2011 Physics of Plasmas **18** 082507.
- [12]. J. Lee et al., 2012 Plasma Physics and Controlled Fusion **54** 125005.
- [13]. Xiaoyin Guan et al., 2013 Physics of Plasmas **20** 022502.
- [14]. J.E. Rice et al., 2011 Nuclear Fusion **51** 083005.
- [15]. J.E. Rice et al., 2011 Physical Review Letters **107** 265001.
- [16]. J.E. Rice et al., 2012 Physics of Plasmas **19** 056106.
- [17]. A. Bortolon et al., 2006 Physical Review Letters **97** 235003.
- [18]. P.H. Diamond et al., 2009 Nuclear Fusion **49** 045002.
- [19]. Ö.D. Gürçan et al., 2007 Physics of Plasmas **14** 042306.
- [20]. Y.Kosuga et al., 2010 Physics of Plasmas **17** 102313.
- [21]. Ö.D. Gürçan et al., 2010 Physics of Plasmas **17** 112309.
- [22]. J.E. Rice et al., 2011 Physical Review Letters **106** 215001.
- [23]. J. Ko et al., 2010 Review of Scientific Instruments **81** 033505.
- [24]. S. Shiraiwa et al., 2011 Physics of Plasmas **18** 080705.
- [25]. L. Wang and P.H. Diamond, 2013, 'Gryokinetic theory of turbulent acceleration of parallel rotation in tokamak plasmas', submitted to Physical Review Letters.
- [26]. J.M. Kwon et al., 2012 Nuclear Fusion **52** 013004.
- [27]. S.Yi et al., 2012 Physics of Plasmas **19** 112506.
- [28]. S.Yi et al., 2013, submitted to Nuclear Fusion.

	sawteeth	no sawteeth
co-	0	89
counter-	146	8

Table 1: Number of discharges, showing correlation between sawteeth and rotation increment direction with LHCD for low density L-mode target plasmas from C-Mod.

Device	ΔV	$n_e(10^{20}/m^3)$	q_{95}	s.t.	I(MA)	B(T)	R(m)	Ref.
C-Mod	counter	0.6–1.2	<5	y	0.8	5.4	0.67	[5, 6, 9]
C-Mod	co	0.4–0.6	6–10	n	<0.6	5.4	0.67	[9]
EAST	co	0.08	10	n	0.25	2	1.8	[8]
JET	co	0.20	4.4	n	2	2.8	2.96	[7, 10]
JET	counter	0.21	4.1	y	2	2.5	2.96	[10]
JT-60U	co	0.04	6.2	n	1.2	3.6	3.4	[4]
Tore Supra	co	0.47	3.9	n	0.7	2.2	2.34	
Tore Supra	counter	0.58	3.9	y	1.2	3.9	2.34	

Table 2: Machine and operational parameters for LHCD experiments in L-mode plasmas on various devices. The column marked s.t. indicates whether or not there were sawtooth oscillations.

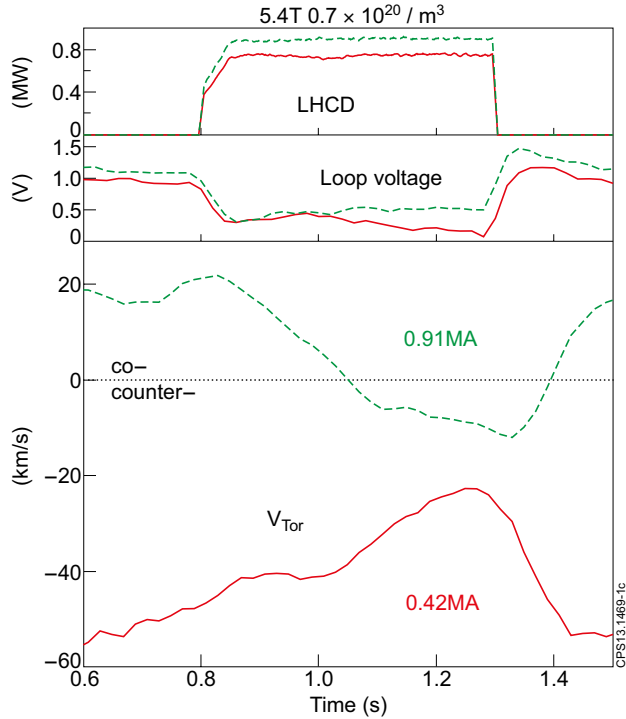


Figure 1: Time histories of the LHCD power, loop voltage and core toroidal rotation velocity for 5.4T discharges from Alcator C-Mod, with plasma currents of 0.91MA (green dashed line) and 0.42MA (solid red line).

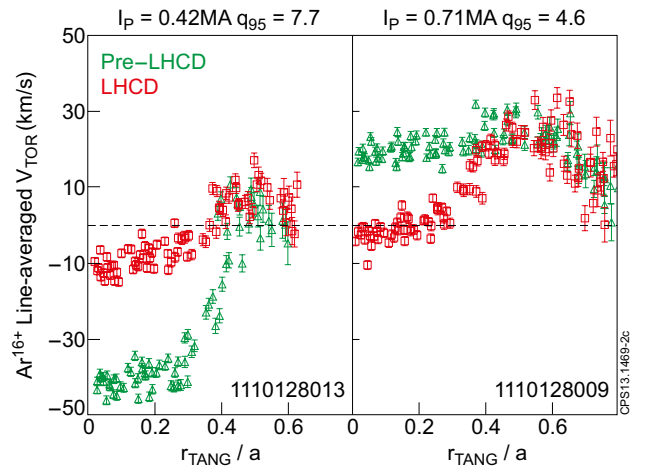


Figure 2: Toroidal rotation spatial profiles before (green) and during (red) LHCD for 0.42MA (left) and 0.71MA (right) discharges.

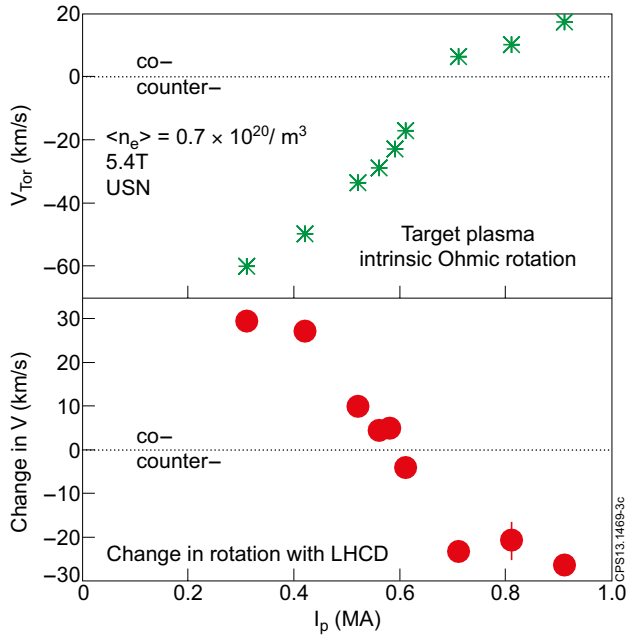


Figure 3: The core toroidal rotation velocity as a function plasma current for 5.4T USN discharges with $n_e = 0.7 \times 10^{20} / m^3$, during the Ohmic phase before LHCD (top). The change in the central toroidal rotation velocity during LHCD as a function of plasma current (bottom).

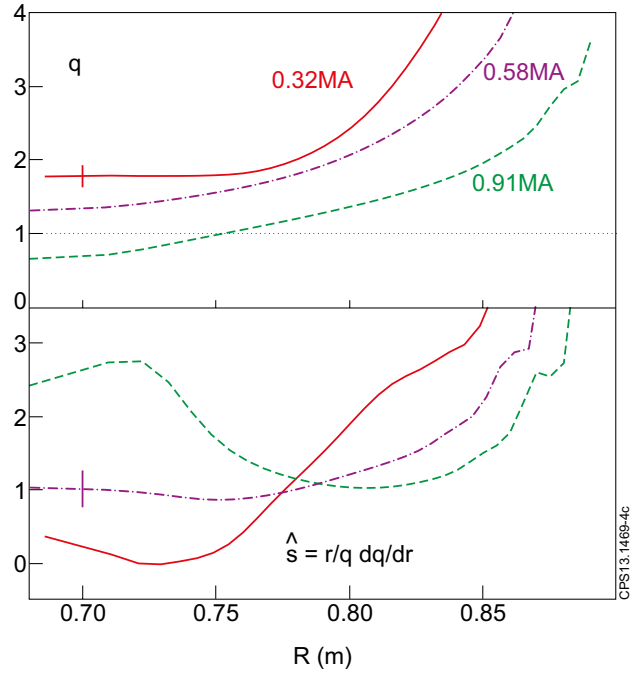


Figure 4: The rotational transform q (top) and magnetic shear (bottom) profiles for 0.32MA (red solid), 0.58MA (purple dash-dot) and 0.91MA (green dashed) discharges with LHCD. Typical error bars are shown.

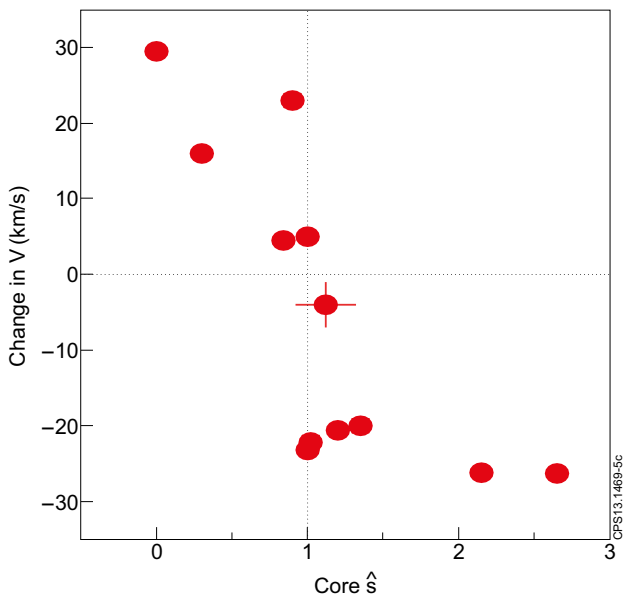


Figure 5: The change in the core rotation velocity with LHCD as a function of the core magnetic shear.

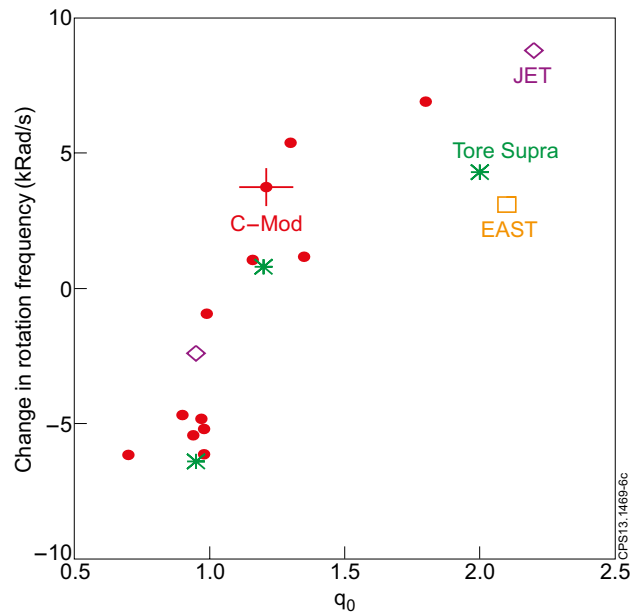


Figure 6: The change in the core rotation frequency with LHCD as a function of q_0 . Dots: C-Mod, asterisks: Tore Supra, diamonds: JET, box: EAST.